Pore-size dependence of rotational tunneling in confined methyl iodide

R. M. Dimeo,[1] D. A. Neumann,[1] Y. Glanville,[2] and D. B. Minor[3]
[1]*NIST Center for Neutron Research, National Institute of Standards and Technology, Gaithersburg, Maryland 20899*
[2]*Department of Physics, The Pennsylvania State University, University Park, Pennsylvania 16802*
[3]*NIST Ceramics Division, National Institute of Standards and Technology, Gaithersburg, Maryland 20899*
(Received 6 June 2002; revised manuscript received 18 July 2002; published 10 September 2002)

High resolution inelastic incoherent neutron scattering measurements have been performed on methyl iodide, a quantum rigid rotor, confined to porous silica glasses with varying pore size distributions. A simple geometrical model composed of weakly and strongly disordered molecules is applied to describe the disordered tunneling molecules, and it is found that the strongly disordered rotors are constrained to three molecular layers. No simple relationship is found between the pore size distribution and the barrier height distribution, thus suggesting that the tunneling line shape cannot be expressed as a simple integral over the pore size distribution.

DOI: 10.1103/PhysRevB.66.104201 PACS number(s): 61.43.Gt, 29.30.Hs, 61.12.−q

I. INTRODUCTION

The presence of structural disorder can have a dramatic effect on macroscopic material properties. At the atomic scale, structural disorder is typically described in terms of distributions of geometrical quantities such as bond lengths and bond angles that are determined from diffraction measurements. Alternatively, disorder can be quantified by determining the distribution of potential energies experienced by the atomic scale constituents of the system. For a highly ordered (crystalline) system the distribution is sharp, while it is broad for a disordered system. Rotational tunneling spectroscopy is a useful tool for characterizing the local molecular environment due to its exquisite sensitivity to the local potential.[1] Here we report high resolution inelastic neutron scattering measurements of methyl iodide adsorbed in a series of porous silica glasses, and relate the degree of confinement-induced disorder in the methyl iodide to the distribution of pore sizes in the glass.

There are several characteristics of porous glasses that can potentially influence confinement-induced disorder, and therefore the dynamics, of an adsorbate. For example, the presence of hydroxyl (OH) groups on the surfaces of porous silica will undoubtedly influence the static structure, particularly for a polar adsorbate such as methyl iodide (CH_3I). Raman and optical Kerr effect spectra indeed show differences in the dynamics of liquid methyl iodide adsorbed in porous systems with differing surface treatments.[2–4] Moreover, rotational tunneling measurements reveal less disorder for CH_3I adsorbed in a porous glass with a hydrophobic surface, compared to one with a hydroxylated surface.[5] Surface roughness can also play a role in the adsorbate dynamics as has been observed for H_2 in porous Vycor glass.[6]

There are three geometrical characteristics of the pores themselves that may influence the adsorbate: the mean pore size, the width of the pore size distribution, and the shape of the pores. Of these, previous investigations of the dynamics of confined materials have generally focused on the average pore diameter. Thus the porous hosts were chosen to have narrow pore size distributions. For example, inelastic neutron scattering has been used extensively to study the effects of pore size on the rotational excitations in methane confined in a range of systems including dodecasil 3C, silica gels, controlled-pore glasses, and MCM-41, all of which had narrow pore size distributions.[7,8] However many practical porous systems have a pore size distribution with a significant width. Furthermore it seems that the degree of disorder and therefore the dynamics of the adsorbate should depend on the width of the pore size distribution of the host. In this study, we examine how the pore size distribution affects the orientational barrier distribution extracted from the tunneling spectra of CH_3I.

The rotational dynamics of methyl groups can often be understood using a simple single-particle model in which motion is hindered by a threefold symmetric orientational barrier.[1,9] The Hamiltonian for the methyl dynamics can then be expressed as

$$H = -B\frac{d^2}{d\phi^2} + \frac{V_3}{2}(1-\cos 3\phi), \tag{1}$$

where B is the rotational constant for the methyl group (655 μeV), V_3 is the height of the hindering barrier, and ϕ is the angular coordinate of the methyl group. If the barrier is not too large, the wave functions will have significant overlap and quantum mechanical tunneling between the minima can occur at low temperature. Moreover, the energy splitting (i.e., tunneling frequency) depends approximately exponentially on the value of V_3. Thus measurements of the tunneling energy are extremely sensitive to the distribution of local environments. CH_3I is a particularly good candidate for use as a probe molecule because in the bulk it is a one-dimensional rotor for which Eq. (1) applies very well. The tunneling spectrum in the low temperature solid phase displays a single sharp tunneling peak at an energy transfer of 2.4 μeV (0.6 GHz) corresponding to a barrier height of 42 meV.[10] This makes the data analysis quite straightforward.

Although CH_3I appears to be an ideal adsorbate to use as a probe molecule, there are few previous measurements of confined solid CH_3I. Inelastic neutron scattering measurements of the low energy dynamics have shown that when CH_3I is confined to a porous glass having a diameter 5.8 nm,

the tunnel spectrum consists of three components: a set of resolution-limited bulklike peaks at ± 2.4 μeV, somewhat broadened tunneling peaks at about ± 4 μeV, and a very broad component attributed to tunneling methyl groups under the influence of a broad distribution of barrier heights.[11] Based on measurements of the CH_3I concentration dependence, these components have been assigned to methyl groups at the center of the pore, near the center of the pores, and near the pore walls, respectively. Measurements of confined CH_3I have also been performed in the liquid state. Optical Kerr effect measurements have revealed two relaxation times, the slower component arising from the molecules near the pore walls.[4] Raman experiments show that the linewidth of the ν_2 vibration (the *umbrella* mode of the methyl group) increases as the pore radius decreases.[2,3] In these light scattering studies, the porous hosts were fabricated to have a narrow pore size distribution in an effort to minimize the effects of the pore size distribution from the measured dynamics.

II. EXPERIMENTAL DETAILS

The porous materials used in this investigation were Geltech-75, Geltech-200, and silica xerogel (manufactured by PQ Corporation under the product name Britesorb).[12] The Geltech samples are monolithic disks 6 mm in diameter and 2 mm thick. The xerogel is a silica powder with a mean particle size of 11 μm.[13,14] The characterization of the porous hosts was performed via nitrogen adsorption/desorption isotherm measurements using a Quantachrome Autosorb Gas Adsorption System.[12] The pore size distributions for each of these materials as determined via the desorption branch of the isotherm were analyzed using the Kelvin equation which assumes a cylindrical pore geometry.[17] In all three porous samples the adsorption/desorption curves were consistent with a distribution of cylindrical pores. The resulting pore size distributions are shown in Fig. 1. The surface area [determined via multipoint BET (Ref. 17)], mean pore diameter $\langle d \rangle$, and standard deviation σ_{PSD} (determined by a fit of the distributions to a Gaussian) are listed in Table I.[15] Based on the values of σ_{PSD} we conclude that the xerogel is the most disordered of the three hosts.

The porous hosts were prepared so that approximately 95% of the pore volume was filled with CH_3I. The details of the sample preparation have been described elsewhere, so they will not be repeated here.[11] The porous glass surfaces were not treated so it is likely that OH groups were present. All neutron scattering measurements were carried out at the NIST Center for Neutron Research with the NIST high-flux backscattering spectrometer.[18] The instrument was operated with a dynamic range of ± 11 μeV (energy transfer) and an energy resolution (full width at half maximum) of 0.79 μeV. In each measurement the samples were contained in a thin-walled aluminum sample can mounted in a top-loading helium flow cryostat and controlled at a temperature of 5 K.

The spectra collected at a wavevector transfer of 1.42 Å^{-1}, normalized to the incident beam monitor, are shown in Fig. 2. The data were fit with a simple model that describes methyl rotor tunneling dynamics under the influence of a

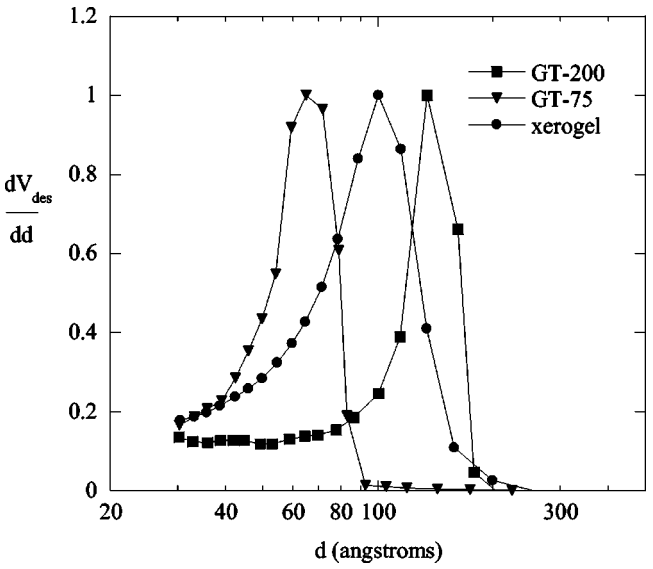

FIG. 1. Pore size distributions as determined using nitrogen adsorption/desorption measurements. Distribution maxima have been normalized to unity. Solid lines connect the points.

distribution of barrier heights. Such models have been used extensively to model the behavior of disordered tunneling systems[19–21] and confined tunneling dynamics.[6–8,11,22,23] The function used to model the scattering intensity is

$$I(Q,E) = I_o \int g(V_3) S_{MG}^{inc}(Q,E,V_3) dV_3, \tag{2}$$

where $S_{MG}^{inc}(Q,E,V_3)$ is the incoherent scattering function for the methyl group, I_o is the integrated intensity, and $g(V_3)$ is a distribution of barrier heights. At low temperature, the incoherent scattering function is given by

$$S_{MG}^{inc}(Q,E) = \frac{5+4j_o(Qr)}{9}\delta(E) + \frac{2[1-j_o(Qr)]}{9}[\delta(E+E_t)+\delta(E-E_t)], \tag{3}$$

where r is the radius of the methyl group, j_o is the zeroth order spherical Bessel function, and E_t is the energy transfer corresponding to the tunneling frequency.[1] The dependence of the tunneling energy E_t on the barrier height is determined from the Hamiltonian [Eq. (1)], for a broad range of barrier heights. To a good approximation the barrier height distribution, $g(V_3)$ can be modeled with two Gaussian distributions which we parametrize as follows:

$$g(V_3) = \sum_{i=1}^{2} \frac{f_i}{\sqrt{2\pi\sigma_i^2}} \exp\left[-\frac{1}{2}\left(\frac{V_3 - v_{3,i}}{\sigma_i}\right)^2\right]. \tag{4}$$

Since the ground state tunneling transition is approximately exponentially dependent on the barrier height, a symmetric distribution of barrier heights, such as a Gaussian, leads to an asymmetric tunneling line shape.[6–8,11,19–23] Based on previous work, the narrow Gaussian component can be attributed

TABLE I. Characterization of porous materials and summary of fit results. SA denotes the specific surface area, $\langle d \rangle$ is the mean of the pore size distribution, σ_{PSD} is the standard deviation, and the other model parameters are described in the text.

sample	SA (m^2/g)	$\langle d \rangle$ (nm)	σ_{PSD} (nm)	$v_{3,1}$ (meV)	σ_1 (meV)	$v_{3,2}$ (meV)	σ_2 (meV)	f_2
GT-25 (Ref. 5)	525	2.7	0.66	N/A	N/A	39.6(3)	6.6(3)	1
GT-50 (Refs. 11,15 and 16)	504	5.8	1.7	37.3(1)	1.29(9)	36.6(3)	6.1(3)	0.75(3)
GT-75	464	6.5	3.0	38.6(1)	1.11(9)	38.7(3)	5.5(3)	0.63(4)
GT-200	215	14.4	4.5	39.22(2)	1.24(3)	37.9(3)	5.9(3)	0.36(1)
xerogel	402	10.0	7.6	39.8(4)	1.9(1)	38(1)	9(1)	0.43(4)

to CH_3I molecules near the center of the pore while the broad component arises from those molecules near the pore walls.[11] The previous measurements also revealed a small sharp bulklike component. We believe that this is because the weakly disordered peaks for CH_3I in the 5.8-nm pores were better separated from the bulklike peaks thus allowing the bulklike peaks to be observed. In fitting the data, the amplitudes (f_i), centers ($v_{3,i}$), and widths (σ_i) of the two distributions were allowed to vary. A comparison of least-squares fits of this model (convoluted with the instrumental resolution function) to the data are shown as the solid lines in Fig. 2. The dashed lines represent the individual components.

III. RESULTS AND DISCUSSION

The pore-size dependence of the integrated intensity of the inelastic features associated with the weakly disordered (fraction f_1) and strongly disordered molecules (fraction f_2) can provide quantitative information on the number of molecular ''layers'' associated with each component. Figure 3 shows that the fractional intensity f_2 for the strongly disordered component decreases as the pore size increases.

A simple two-component model can account for the pore size dependence of f_2. Assume that the strongly disordered molecules are constrained to a thickness t on the pore walls, and that the pore radii are uniform (see the inset of Fig. 3). For a mean pore diameter $\langle d \rangle$ the fraction in the layer thickness, t, is given by

$$f_2 = 2\left(\frac{2t}{\langle d \rangle}\right) - \left(\frac{2t}{\langle d \rangle}\right)^2 \tag{5}$$

for $\langle d \rangle \geq 2t$. The fit of Eq. (5) to the data in Fig. 3 yields a thickness of $t = 1.41 \pm 0.04$ nm. Assuming bulk density for the confined CH_3I, this corresponds to about three molecular layers consistent with previous measurements.[11] The model also predicts that f_2 will approach unity as the diameter approaches twice the thickness ($2t = 2.82$ nm). This is consistent with our previous measurements[5,11] which are also

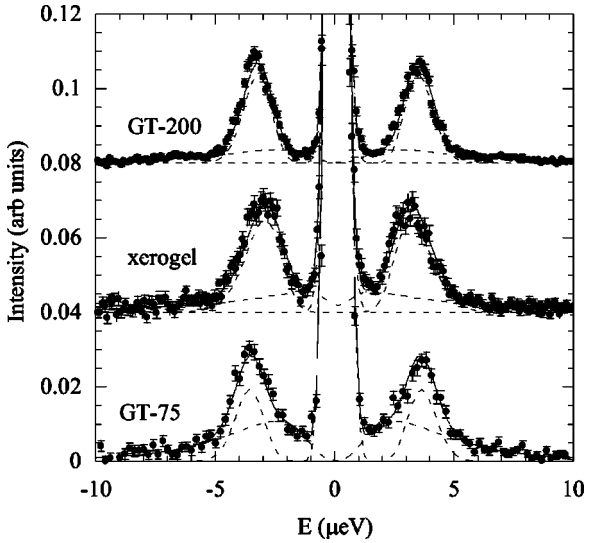

FIG. 2. Rotational tunneling spectra for CH_3I in the three porous materials at a wave-vector transfer of 1.42 $Å^{-1}$. The solid line is a fit described in the text, and the dashed lines are the individual components. Note that the relative intensities of the two components depend on the pore diameter, but that the peak positions and widths of the tunneling lines do not change monotonically with the average pore size.

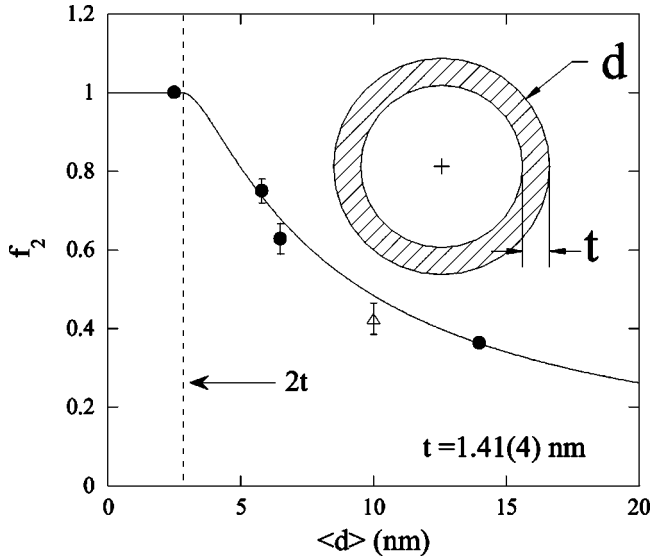

FIG. 3. Fraction of the disordered integrated intensity f_2 as a function of the mean pore diameter. The solid line is a fit to the model discussed in the text. The dashed line is drawn at twice the disordered layer thickness. The inset shows the simple geometrical picture used in the model. The hatched region signifies the strongly disordered molecular thickness. Solid symbols represent measurements in Geltech, and the open symbol is for xerogel.

shown in Fig. 3. This thickness is comparable with that of the surface layer of methane, 2.0 ± 0.5 nm, in controlled-pore glasses[8] whereas the bulklike behavior of methane on the crystalline surface MgO is observed when four such layers are adsorbed.[24] Furthermore, x-ray scattering measurements of water at an electrode-electrolyte interface show that the effects of the fields at the surface extend out to three molecular layers.[25] Fits were also made to the present data using the integral of Eq. (5) over the pore size distributions. Within the uncertainty the resulting thickness is the same as obtained by fitting Eq. (5). Thus the relative amplitude of the two components is primarily determined by $\langle d \rangle$ rather than the width of the pore size distribution.

Previous Raman measurements of confined liquid CH_3I show that the ν_2 vibrational peak shifts to lower energy as the mean pore diameter decreases.[2] Extrapolating the trend observed in the Raman measurements for this motion which occurs along the I-C axis to rotational motions about the I-C axis would lead one to expect the barrier height to be a monotonically decreasing function of the mean pore size. Furthermore, the sharper component of $g(V_3)$ in the confined CH_3I reflects a smaller hindering potential than found for the bulk also suggesting that the barrier should decrease as $\langle d \rangle$ decreases. Taken together, these results suggest that the scattering intensity can be expressed as

$$I(Q,E) = I_o \int P(D) S_{MG}^{inc}(Q,E,V_3,D) dD, \tag{6}$$

where $P(D)$ is the pore size distribution, $V_3 = V_3(D)$ is a monotonically decreasing function of pore diameter, and the rest of the equation has been explained in reference to Eq. (3). Note that the assumption implicit in Eq. (6) is that the barrier height distribution $g(V_3)$ can be expressed in terms of the pore size distribution $P(D)$ via

$$g(V_3) = P(D) \left| \frac{\partial V_3}{\partial D} \right|^{-1}. \tag{7}$$

The relationship between the widths of the barrier height distribution, σ_{V_3}, and those of the pore size distribution, σ_{PSD}, is also implicit in Eq. (6):

$$\sigma_{V_3} = \left| \frac{\partial V_3}{\partial D} \right| \sigma_{PSD}. \tag{8}$$

While the relative intensity of the two tunneling features we observe can be simply described using just the mean pore diameter, neither the peak positions nor the widths display a monotonic dependence on the mean pore diameter (see Table I). Thus these measurements show that, unlike the intensities of the two components, there is no simple correlation between the mean of the pore size distribution and the mean of $g(V_3)$, i.e., a single pore diameter does not necessarily correspond to a single barrier height. Similar arguments apply to the relative widths of $g(V_3)$. Thus neither the mean nor the width of $g(V_3)$ is a simple monotonic function of $\langle d \rangle$, and Eq. (6) does not appear to be valid.

Figure 4 shows the widths (σ_1, σ_2) of the components of $g(V_3)$ as a function of σ_{PSD}. The width of $g(V_3)$ appears to

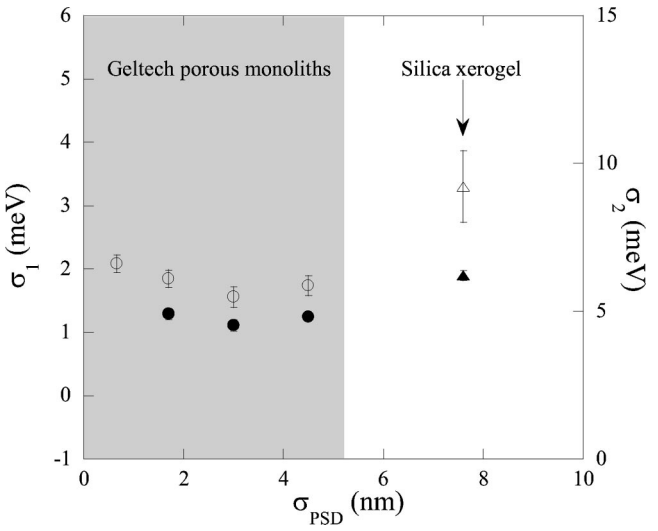

FIG. 4. Widths of the components of $g(V_3)$ as a function of the widths of the pore size distribution. Disordered widths (σ_2) are plotted as open symbols, and the ordered components (σ_1) are represented by the solid symbols.

have only a very weak non-monotonic dependence on the width of the pore size distribution. For CH_3I confined in Geltech, shown in the shaded region in Fig. 4, there appears to be almost no dependence on the distribution width whereas confinement in xerogel results in an increase in the widths of the components of $g(V_3)$. This is consistent with our observation that there is no such dependence of the barrier height positions nor widths on pore diameter since $V_3 = V_3(D)$ necessarily implies that that the widths of the distribution are related via Eq. (8). Therefore $g(V_3)$ cannot be expressed as a simple integral over the pore size distribution.

The fact that both the position and width of the components of $g(V_3)$ in Geltech are nearly constant indicates that the local environment is not dependent on the pore size distribution itself, i.e., the two local structures are nearly independent of the size (local or global) of the pores. This fact is not surprising since we have neglected the effects of surface interactions. Preliminary results on CH_3I in a porous glass with 5.8-nm pores with hydrophobic OCH_3 groups indicate an enhancement of the ordered barrier contribution to the overall barrier height distribution suggesting that the thickness of the strongly disordered surface component is reduced.[5] The surface chemistry, largely dependent on the fabrication process, can be quite different for the Geltech compared to that of the xerogel. This could be the key to the differences in the widths of $g(V_3)$, as shown in Fig. 4. In future studies we intend to treat the surfaces of the porous glasses of varying nominal pore diameters to replace the OH groups thereby changing the surface-adsorbate interactions. This could shed further light on the pore-size dependence of the barrier height distribution as well as the differences seen between the Geltech and the xerogel.

IV. CONCLUSION

In conclusion, we find that the rotational tunneling spectrum for CH_3I confined to porous glasses with various mean

diameters and dispersions can all be treated with a simple two-component model composed of weakly and strongly disordered molecules. Based on this model we estimate that the strongly disordered molecules are constrained to three molecular layers. Furthermore we find that there is no monotonic dependence of the widths of the components of the orientational barrier distribution as extracted from rotational tunneling spectra on the width of the pore size distribution of the porous material in which the CH_3I is adsorbed. Moreover we find no simple correlation between the mean diameter and the barrier height nor do we find a simple correlation between the width of the barrier distribution and the nominal pore diameter. These results taken together indicate that the confined tunneling line shape cannot be expressed as a simple integral over the pore size distribution. Rather surface interactions seem to dominate the local structure and therefore the dynamics of CH_3I in mesoporous glasses.

ACKNOWLEDGMENTS

We are grateful to Professor Paul Sokol of the Pennsylvania State University for useful discussions, and David Silva of the Pennsylvania State University for providing the particle size measurements of the xerogel. This work is based upon activities supported by the National Science Foundation under Agreement Nos. DMR-0086210 and DMR-9970126.

[1] W. Press, in *Single-Particle Rotations in Molecular Crystals* (Springer-Verlag, Berlin, 1981).
[2] Y. T. Lee, S. L. Wallen, and J. Jonas, J. Phys. Chem. **96**, 7161 (1992).
[3] T. R. Bryans, R. E. Wilde, M. W. Holtz, and E. L. Quitevis, Chem. Phys. Lett. **314**, 459 (1999).
[4] B. J. Loughnane and J. T. Fourkas, J. Phys. Chem. B **102**, 10 288 (1998).
[5] R. M. Dimeo and D. A. Neumann, Appl. Phys. A (to be published).
[6] D. W. Brown, P. E. Sokol, and S. A. Fitzgerald, Phys. Rev. B **59**, 13 258 (1999).
[7] D. Balszunat, B. Asmussen, M. Muller, W. Press, W. Langel, G. Coddens, M. Ferrand, and H. Buttner, Physica B **185**, 226 (1996).
[8] C. Gutt, B. Asmussen, I. Krasnov, W. Press, W. Langel, and R. Kahn, Phys. Rev. B **59**, 8607 (1999).
[9] M. Prager and A. Heidemann, Chem. Rev. **97**, 2933 (1997).
[10] M. Prager, J. Stanislawski, and W. Hausler, J. Chem. Phys. **86**, 2563 (1987).
[11] R. M. Dimeo and D. A. Neumann, Phys. Rev. B **63**, 014301 (2001).
[12] Manufacturers are identified in order to provide complete identification of experimental conditions, and such identification is not intended as a recommendation or endorsement by NIST.
[13] D. E. Silva (private communication).
[14] K. A. Berg, R. H. Witt, and R. Derolf, Beer Processing and Composition, Pennsylvania, U.S. Patent No. 5,149,553 (1991).
[15] The pore size distribution for the material used in Ref. 11 has been calculated based upon a reanalysis of the adsorption/desorption isotherm data consistent with the method applied to the new materials reported here. These results of the characterization differ somewhat from those reported in Ref. 11.
[16] A more careful description of the resolution used in fitting the tunneling spectra in Ref. 11 yields a smaller intrinsic width of the disordered component of $g(V_3)$ than originally reported. The value of the disordered width, σ_2, is particularly sensitive to the scattering intensity close to the elastic peak so a careful characterization of the resolution function is necessary.
[17] D. D. Do, in *Adsorption Analysis: Equilibria and Kinetics* (Imperial College Press, London, 1998).
[18] P. M. Gehring and D. A. Neumann, Physica B **241-243**, 64 (1998).
[19] S. Grondey, M. Prager, W. Press, and A. Heidemann, J. Chem. Phys. **85**, 2204 (1986).
[20] C. Bostoen, G. Coddens, and W. Wegener, J. Chem. Phys. **91**, 6337 (1989).
[21] J. Colmenero, R. Mukhopadhyay, A. Alegria, and B. Frick, Phys. Rev. Lett. **80**, 2350 (1998); A. J. Moreno, A. Alegria, J. Colmenero, M. Prager, H. Grimm, and B. Frick, J. Chem. Phys. **115**, 8958 (2001); A. J. Moreno, A. Alegria, J. Colmenero, and B. Frick, Macromolecules **34**, 4886 (2001); Phys. Rev. B **65**, 134202 (2002).
[22] J. M. Nicol, J. Eckert, and J. Howard, J. Phys. Chem **92**, 7117 (1988).
[23] M. Bienfait, B. Asmussen, P. Zeppenfeld, W. Press, J. P. Palmari, M. Johnson, C. Journet, P. Bernier, K. Meternier, S. Bonnamy, and N. Dupont-Pavlowski, Physica B **301**, 292 (2001).
[24] J. Z. Larese, D. Martin y Marero, D. S. Sivia, and C. J. Carlile, Phys. Rev. Lett. **87**, 206102 (2001).
[25] M. F. Toney, J. N. Howard, J. Richer, G. L. Borges, J. G. Gordon, O. R. Melroy, D. G. Weisler, D. Yee, and L. B. Sorensen, Nature (London) **368**, 444 (1994).